catalysts

MDPI

Article

Immobilization-Stabilization of β-Glucosidase for Implementation of Intensified Hydrolysis of Cellobiose in Continuous Flow Reactors

Celia Alvarez-Gonzalez, Victoria E. Santos, Miguel Ladero * and Juan M. Bolivar *

FQPIMA Group, Chemical and Materials Engineering Department, Faculty of Chemical Sciences, Complutense University of Madrid, 28040 Madrid, Spain; cealva03@ucm.es (C.A.-G.); vesantos@ucm.es (V.E.S.)
* Correspondence: mladero@quim.ucm.es (M.L.); juanmbol@ucm.es (J.M.B.)

Abstract: Cellulose saccharification to glucose is an operation of paramount importance in the bioenergy sector and the chemical and food industries, while glucose is a critical platform chemical in the integrated biorefinery. Among the cellulose degrading enzymes, β-glucosidases are responsible for cellobiose hydrolysis, the final step in cellulose saccharification, which is usually the critical bottleneck for the whole cellulose saccharification process. The design of very active and stable β-glucosidase-based biocatalysts is a key strategy to implement an efficient saccharification process. Enzyme immobilization and reaction engineering are two fundamental tools for its understanding and implementation. Here, we have designed an immobilized-stabilized solid-supported β-glucosidase based on the glyoxyl immobilization chemistry applied in porous solid particles. The biocatalyst was stable at operational temperature and highly active, which allowed us to implement 25 °C as working temperature with a catalyst productivity of 109 mmol/min/$g_{support}$. Cellobiose degradation was implemented in discontinuous stirred tank reactors, following which a simplified kinetic model was applied to assess the process limitations due to substrate and product inhibition. Finally, the reactive process was driven in a continuous flow fixed-bed reactor, achieving reaction intensification under mild operation conditions, reaching full cellobiose conversion of 34 g/L in a reaction time span of 20 min.

Keywords: cellulose hydrolysis; β-glucosidase immobilization; enzyme immobilization; kinetic modelling; reactor engineering; flow biocatalysis

Citation: Alvarez-Gonzalez, C.; Santos, V.E.; Ladero, M.; Bolivar, J.M. Immobilization-Stabilization of β-Glucosidase for Implementation of Intensified Hydrolysis of Cellobiose in Continuous Flow Reactors. *Catalysts* **2022**, *12*, 80. https://doi.org/10.3390/catal12010080

Academic Editor: Martina Letizia Contente

Received: 28 November 2021
Accepted: 5 January 2022
Published: 11 January 2022

1. Introduction

While global demand for energy and material resources is increasing, the environmental impact due to the extraction, transport, transformation, and use of fossil resources poses a critical challenge to humanity, affecting our environment even at global scale. In such a situation, there is an urgent need to create very efficient strategies to obtain goods and services and to use them in a sustainable way, creating cycles of extraction, creation, and utilization in what is named the circular economy [1–4]. The nature of resources is a key aspect: they should be renewable. Lignocellulosic biomass is very plentiful, ubiquitous, and available. The nature of processes is also critical: they should be exquisite in the transformation of resources into useful products, avoiding residues and energy losses. Processes based on biocatalysts (enzymes, cells) are run in very mild conditions (T, P), while enzymes can exhibit an almost perfect selectivity for substrates and reactions. The combination of the renewable and available nature of lignocellulosic resources with depolymerizing and saccharifying enzymes is a critical stage in the upstream section of lignocellulose-based biorefineries [2,3]. However, previously, pretreatments based on heat, mechanical forces, acid, and basis reagents and/or solvents are needed to attain the adequate accessibility and reactivity of the target solid substrate, rich in cellulose. Such cellulose will be the target for the action of depolymerising (endo- and exoglucanases and lytic polysaccharide

monooxygenases -LPMOs-) and saccharifying enzymes (β-glucosidases), aided by other hydrolases acting on remaining hemicellulose and pectin, and other proteins disrupting the crystal structure of cellulose (swollenins, expansins) [5,6].

Glucose, a key C6 platform chemical in biorefineries, is mainly obtained through the hydrolyzing action of β-glucosidases of fungal and bacterial origin, either acting as free proteins or as part of a cellulosome [5]. Three different kinds of enzymes take part in the enzymatic breakdown and depolymerization of cellulose: endoglucanases, exoglucanases, and β-glucosidases. β-glucosidases (β-D-glucoside glucohydrolase, EC 3.2.1.21) belong to the glycoside hydrolase family, and they can hydrolyze O- or S- glycosidic bonds at the non-reducing end of polysaccharides, oligosaccharides, and glucosides, thus releasing β-D-glucopyranose. Its main role in biomass saccharification is the hydrolysis of cellobiose and other cellooligosaccharides (COS) originated during cellulose depolymerization, which constitute glucanase inhibitors. Theirs is a synergistic action with depolymerizing enzymes to avoid or mitigate product inhibition over the diverse enzymatic routes leading to glucose. Curiously, we find in nature β-glucosidases that are devoid of the classical cellulose binding domain (CBM) typical in exoglucanases for example, but others have this binding domain [7], suggesting that they can immobilized near the source of cellobiose and cellooligosaccharides of low molecular weight that are their substrates [8] while possibly benefitting from the stabilizing environment created by the confinement near the surface of the reacting solid substrate [9,10].

β-glucosidases are, in many cases, the main bottleneck in the hydrolysis process of cellulose since cellobiose is a known inhibitor of exo- and endoglucanases. The identification of suitable β-glucosidases, cost-efficient production, catalyst design, and reaction system implementation have received considerable attention [11,12]. Despite the advances, the demands of efficient lignocellulosic biomass valorization, and the valuable application of β-glucosidases in transglycosylation reactions, some [13] have taken an additional technological interest and undertaken research efforts to obtain a suitable β-glucosidase catalyst integrated in practical reaction systems [14–16].

One strategy to facilitate the effective β-glucosidase implementation is the design and implementation of the enzyme in the format of enzyme-immobilized preparations [17,18]. Enzyme immobilization is an enabling technology that facilitates enzyme handling, permits its cyclic reuse and continuous use, and, if properly designed, might contribute to increasing the operational stability of the enzyme [19,20]. Immobilization design involves the choice of material support (where the enzyme is immobilized), the immobilization chemistry and the conditions of immobilization [19,21–23]. As a result, different properties can be modulated suited for applications, e.g., reactor format suitability, activity, stability, and practical use. Therefore, it is not surprising that many examples of β-glucosidase immobilization can be found in literature. Studies mainly involve the immobilization into preexisting materials and the evaluation of the influence of the material supports in the interplay with different immobilization chemistries. Catalytic properties as recovered activity and stability were evaluated [18–26]. Active immobilization by adsorption (anion exchange based ionic adsorption) or covalent binding (via aldehyde chemistry) to porous material supports have been shown as a promising strategy to obtain active and stable catalysts of different β-glucosidases. In these previous works, the focus of the immobilization design was obtaining high specific activity (similar to the free enzyme) and enhancing the stability under resting conditions, which represents a promising point for implementation [17,18,24–32].

The practical application of immobilized β-glucosidases catalysts requires further consideration and the filling of several research gaps. Indeed, the knowledge of activity and stability under resting conditions is not sufficient to have a comprehensive view of the potential of the catalyst. While this is of general interest for diverse biocatalytic systems, it becomes urgent in the case of cellobiose hydrolysis by these enzymes. Reaction time courses are affected by complex kinetics that involve different inhibition issues and inactivation routes. Regarding the kinetics, different approaches for the obtention of representative kinetic models have been used for β-glucosidases. Recently, mixed inhibition models that

involve both substrate inhibition and product inhibition have been elucidated. Mateusz and co-workers analyzed the kinetic behavior of a commercial BG preparation. They tested it for different biocatalyst concentration, different initial substrate, and product concentration in the reaction media. The kinetic model that they propose explains the kinetic through a mixed inhibition model which involves an uncompetitive inhibition by the substrate and double competitive inhibition exerted by the product [33]. Regarding stability, given the natural function of the enzyme of working in the proximity of macromolecular substrates, operational stability might significantly differ from the one studied under resting conditions, using the free enzyme as a standard comparison. Therefore, every solid-supported enzyme formulation has to be specifically addressed regarding kinetic and stability [10,18,33–35].

Motivated by the potential of enzyme immobilization and the special features of the cellobiose hydrolysis, in the present manuscript, we have interfaced enzyme immobilization with chemical reaction engineering with the aim of understanding the catalyst productivity in the interplay of the enzyme kinetics and reactor set-up. Chemical reaction engineering enables the elucidation of the reaction kinetics based on the determination of the fundamental influencing variables and their effects on the temporal evolution of a reacting system [36]. The understanding of enzyme kinetics is needed to unveil the potential of enzymes to satisfy determined production targets and for the design of the reactor. Recently, (bio)catalysis is very much in line with a paradigm shift involving process intensification and the transition from batch to flow reactors [36]. In this regard, chemical reaction engineering tools applied to the determination of enzyme kinetics are of utmost importance for an optimal exploitation of enzymes via optimization of the biocatalyst and of the operational conditions of such catalysts to enhance process productivity [36]. It is not a surprise that the hydrolysis of cellobiose has also received special recent attention regarding intensification of the reaction and transition to continuous flow operation [37–39].

In this paper, we have designed an immobilized-stabilized solid-supported β-glucosidase in porous solid particles. Maximization of the catalytic productivity was assessed by studying the effect of the enzyme loading into the solid support. Stability of the catalyst was studied under resting conditions and operational conditions. The hydrolysis of the cellobiose was studied in a discontinuous stirred tank reactor, following which a simplified kinetic model was applied to assess the process limitations due to substrate and product inhibition. Finally, the reactive process was driven in a continuous flow fixed-bed reactor.

2. Results and Discussion

2.1. Design of Immobilized Preparations of β-Glucosidase

Biocatalyst design first required an assessment of the features of the commercial enzyme preparation. The free enzyme preparation was characterized regarding enzyme activity and protein concentration. Protein concentration was 84.6 $mg_{protein}/mL$ and the enzymatic activity was 1282 $U_{\_pNPG}/mL$. Combining both results, a specific activity of 15.2 $U_{\_pNPG}/mg_{protein}$ was obtained. This activity value agrees with that reported by other authors for this ASA-1000 β-glucosidase formulation [33].

To identify a suitable immobilization methodology, two carrier materials and three surface activations were implemented. As carrier materials, hydrophilic spherical particles made of cross-linked agarose beads (Ag) [40] and spherical particles made from polymethacrylate Lifetech™ECR8209F (Pur) were chosen [40]. The technical specifications of the material are collected in Table S1. As surface activation, both carrier materials were activated according to reported procedures with amino groups (monoaminoethyl-N-aminoethyl: MANAE), polyethylenemine (PEI), or glyoxyl groups (Gly). MANAE or PEI activation pursues a reversible ionic immobilization based on anionic exchange, whereas glyoxyl activation pursues an irreversible multipoint covalent immobilization [41,42]. The effect of the enzyme load was explored by preparing enzyme catalysts with different offered activity: low load (20 $U_{\_pNPG}/g_{support} \Leftrightarrow 1.32\ mg_{protein}/g_{support}$), medium load (200 $U_{\_pNPG}/g_{support} \Leftrightarrow 13.16\ mg_{protein}/g_{support}$), and high load (2000 $U_{\_pNPG}/g_{support}$

$\Leftrightarrow$ 131.60 $mg_{protein}/g_{support}$). Table 1 shows the results of the immobilization in terms of immobilization yield and activity (see Section 3.5 for details).

Table 1. Characterization of the immobilization of the β-glucosidase on different activated supports. For more details of the immobilization parameters definitions see Section 3.5.

Immobilized Biocatalyst	Activity Offered ($U_{-pNPG}/g_{support}$)	Immobilization Yield (%)	Measured Activity ($U_{-pNPG}/g_{support}$)	Recovered Activity (%)	Effectiveness Factor
Ag-MANAE	19.4	38.5	5.7	29.4	0.76
	193	42.3	28.3	14.7	0.35
	1871	43.2	137	7.3	0.17
Ag-PEI	19.4	100	19.4	103	1.00
	1923	97.7	153	79.6	0.81
	1871	93.6	1111	59.4	0.63
Pur-PEI	19.4	100	14.1	72.6	0.73
	193	89.8	119	61.7	0.69
	1871	57.3	423	22.6	0.39
Ag-Gly 4BCL	286	92.7	119	41.76	0.45
	2127	42.8	159	7.57	0.18
Ag-Gly 6BCL	286	85.6	101	35.2	0.41
	2127	39.2	189	8.86	0.23
Pur-Gly	286	91.8	87.9	30.8	0.33
	2127	39.4	77.7	3.66	0.09

In the case of reversible immobilization, yields close to 100% and high effectiveness factors were obtained for PEI activated carriers. Immobilization in Ag-MANAE displayed a significantly worse performance. When irreversible immobilization was performed, these yields reached around 90% while efficiency factors around 0.45 were obtained for medium loads, but both yield and effectiveness decreased with high enzyme loads. The high immobilization yields on PEI activated materials, even at high offered enzyme loads, could be explained by the high amino group concentration that provides the polymeric coating on the surface of the support. Further, it has been reported in the literature that this type of immobilization does not significantly affect enzyme activity [43,44]. In contrast, covalent immobilization usually implies decrease in the recovered activity and effectiveness factor. The latter is usual since covalent immobilization involves structural changes that affect enzyme activity, which explains the decrease in immobilized activity [19,20]. A decrease of effectiveness at high loading is expected since crowding effects or diffusional restrictions can take place. These results agree with those reported in the literature when the β-glucosidase was immobilized in a similar support (mainly agarose) or similar immobilization chemistry was employed: high immobilization yields and recovered activities were obtained for the reversible immobilization [45–47], while lower yields for irreversible immobilization were attained [45,48]. The choice between PEI-activated and glyoxyl-activated requires further research according to the performance in terms of kinetic, productivity, and operational stability, which was studied, and it is described as follows [17,18].

2.2. Kinetic and Stability Characterization of Immobilized β-Glucosidase

The immobilized enzyme catalysts were studied in terms of kinetics and stability under resting conditions. The activity of β-glucosidase towards the hydrolysis of pNPG was measured at different concentrations of the substrate. Figure 1 shows the results. At low concentrations of pNPG, there is a pronounced positive dependency between enzyme activity and substrate concentration. A maximum enzyme activity is not reached since from a certain substrate concentration, velocity is negatively affected, as may be seen in Figure 1, which is a manifestation of substrate inhibition of both immobilized biocatalyst and free enzyme. Starting the inhibition at low substrate concentrations. The similarity

between the behavior of Ag-PEI biocatalyst and the free enzyme is also expressed in terms of substrate concentration dependency, showing a similar influence of substrate inhibition, while covalently immobilized enzymes show a slight shift of the inhibition to higher substrate concentrations. Similarities between Ag-PEI and free enzyme are ascribed to the nature of the immobilization, as commented.

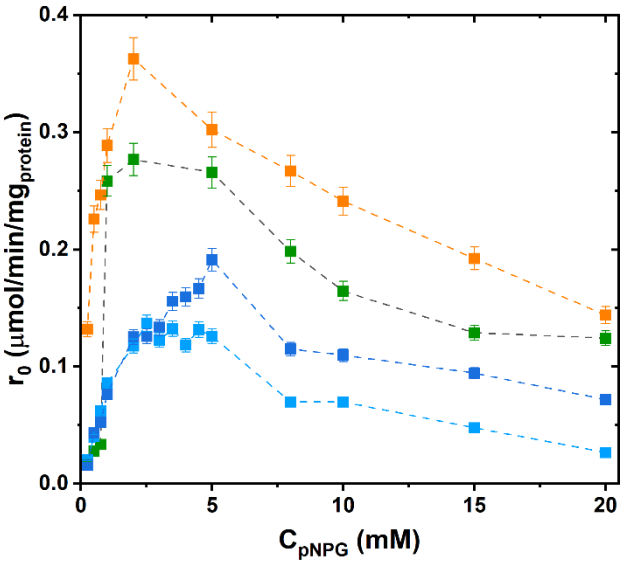

Figure 1. Dependency of the initial rate of pNPG hydrolysis upon substrate concentration variation for different β-glucosidase catalysts. Free enzyme (green) and immobilized enzyme: Ag-PEI 2000 $U_{\_pNPG}/g_{support}$ (orange), Ag-Gly 200 $U_{\_pNPG}/g_{support}$ (light blue) and Ag-Gly 2000 $U_{\_pNPG}/g_{support}$ (dark blue). The data shown are representative of the multiple experiments repeated.

The stability of the immobilized biocatalysts was studied under resting conditions (see Section 3.5 for details). Immobilized biocatalysts were incubated under defined conditions and samples were taken to measure the hydrolytic activity towards pNPG. Results are shown in Figure 2. With respect to the free enzyme, it remained stable at 50 °C (Figure 2A). However, under incubation at 65 °C and 70 °C, protein aggregation and precipitation formation were observed. The formation of enzyme aggregates disabled the determination of the free enzyme activity and the analysis of the monomolecular stability of the enzyme in the homogenous phase [20]. This coincides with reports by other authors that indicate that this enzyme is stable between 40 and 60 °C [27,28,30,49]. Both immobilized biocatalysts were stable for at least 14 days at 50 °C while under incubation at 70 °C they were rapidly deactivated, losing about 80% of activity in one hour (Figure 2B). When incubated at 65 °C (Figure 2C), 25–30% of activity was lost in the early hours. However, the average lifetime was extended up to 40 h and retained approximately 50% of initial activity. This inactivation was fitted to a biexponential (please, see Figure 2C and Table S2, Supplementary Materials) decay with two enzyme population fractions (Table S2, Supplementary Materials). These results showed that the thermal stability was improved with the immobilization. The stability of the biocatalysts at 50 °C is interesting because it is the optimal operating temperature of the β-glucosidase enzyme [10,50] and this also allows comparison with the free enzyme under the same operating conditions when the hydrolysis of cellobiose is implemented.

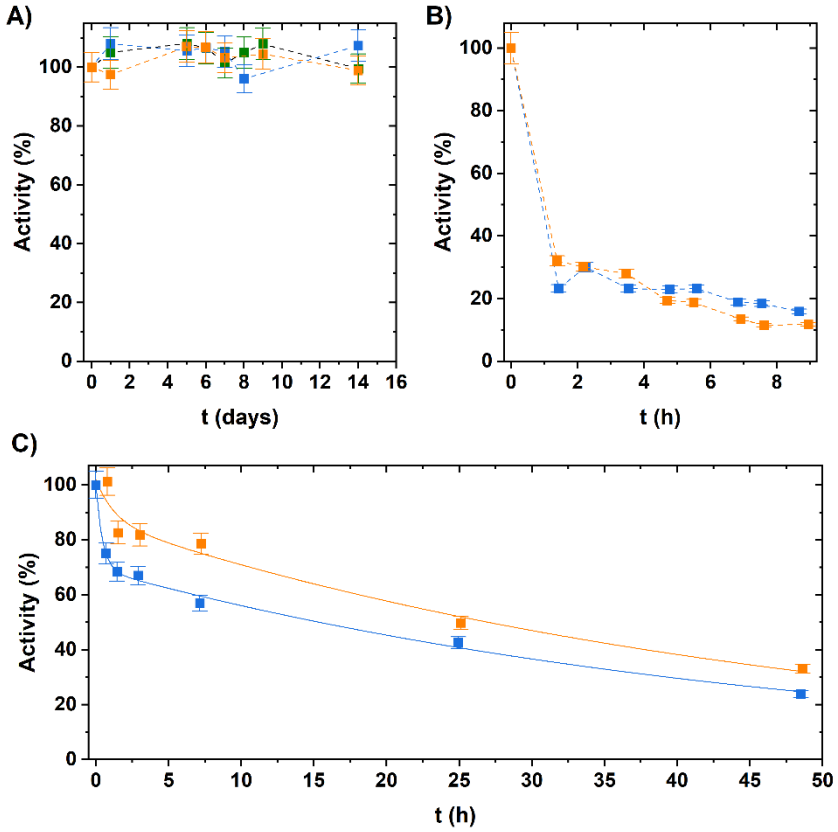

Figure 2. Time course of activity of different enzyme catalysts incubated under resting conditions. Free enzyme (green) and immobilized enzyme: Ag-PEI 2000 $U_{\_pNPG}/g_{support}$ (orange) and Ag-Gly 2000 $U_{\_pNPG}/g_{support}$ (blue). (**A**) T = 50 °C, (**B**) T = 70 °C and (**C**) T = 65 °C. The data shown are representative of the multiple time-course experiments repeated. Continuous line in Panel (**C**) is the line of the biexponential fitting, showing a biphasic inactivation.

2.3. Implementation of the Hydrolysis in Discontinuous Stirred Tank Reactor: Identification of Substrate and Product Inhibition

The hydrolysis of cellobiose catalyzed by immobilized β-glucosidase was implemented in a discontinuous stirred tank reactor in the format of orbitally shaken flasks, as shown in Figure 3. The amount of immobilized enzyme catalyst added to the reactor was set to use an equal amount of enzyme based on the observable activity towards pNPG (Table 1) aiming to employ an enzyme concentration of 0.90 $U_{\_pNPG}/mL$ (Figure 3A) and 4.50 $U_{\_pnPG}/mL$ (Figure 3B). In the timespan of one hour, conversions close to 100% using a cellobiose concentration of 20 g/L were obtained for all the catalysts. The conversion decreased to values of approximately 50% when the cellobiose concentration was 70 g/L, Figure 3A. The increase of the catalyst concentration by a factor of five (Figure 3B) resulted in a clear boost of the initial reaction rate, obtaining conversions close to 100% in only 20 min for low concentrations of cellobiose. In both experiments, the Ag-Gly showed slightly better performance than the Ag-PEI biocatalyst. While a clear boost is observed in the initial reaction rate, the conversion time course significantly slows down, which requires deeper understanding to be able to intensify the reaction.

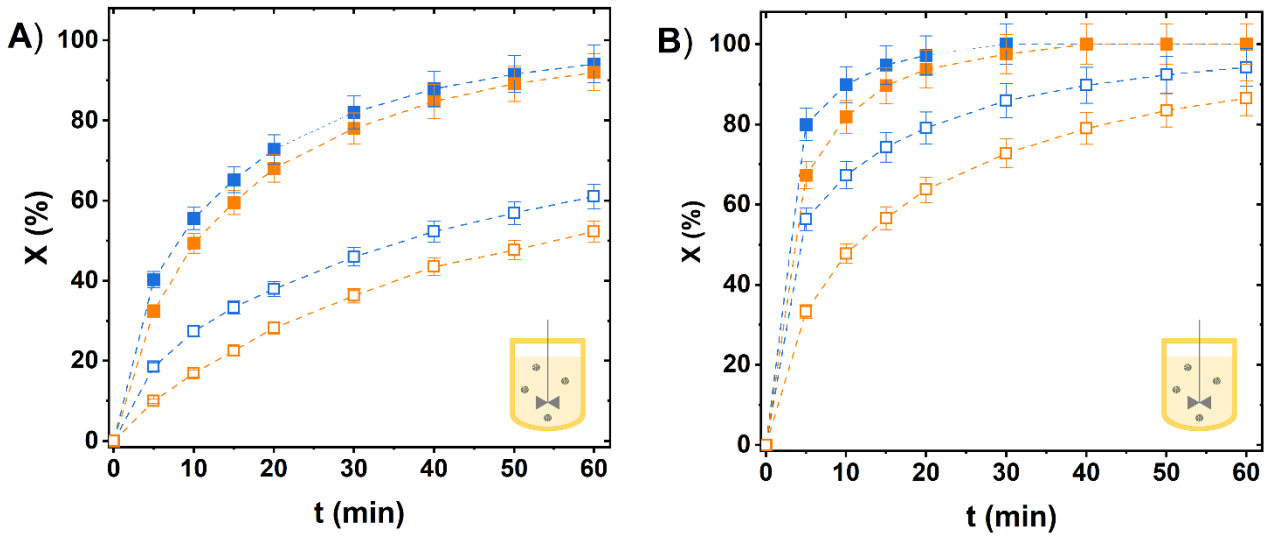

Figure 3. Conversion (X) time course of cellobiose catalyzed by different immobilized biocatalysts: Ag-Gly 2000 $U_{\_pNPG}/g_{support}$ (blue squares); Ag-PEI 2000 $U_{\_pNPG}/g_{support}$ (orange squares) at different enzyme concentrations (**A**) 0.90 $U_{\_pNPG}$/mL and (**B**) 4.50 $U_{\_pNPG}$/mL with different cellobiose concentrations (sodium citrate buffer 50 mM pH 5.0): 20 g/L (filled squares) and 70 g/L (empty squares). The data shown are representative of the multiple time-course experiments repeated. All experiments were performed in batch reactors at 50 °C as reported in the Section 3.6.

To have a better understanding of the factors limiting the hydrolysis of cellobiose, a kinetic analysis was performed by the application of differential and integral calculation methods to the conversion time course. First, we apply the differential calculation method by differentiation of the integral data (Figure 3). The results are shown in Figure 4. Obviously, the reaction rate decreases with time (Figure 4A,B), but the key question is whether this decrease is explained only by cellobiose consumption or if there are other inhibiting or inactivation issues. For that, Figure 4C,D are conceived to provide a useful insight. It is observed that instead of the typical overlapping hyperbolic curves of the characteristic Michaelis–Menten kinetics (proportional to substrate concentration at low substrate concentration, independent from it at very high values of such concentration, where it remains stable), a set of concaves parables is inferred, indicating different reaction rates at the same cellobiose concentration for different experiments performed at different initial cellobiose concentrations, a clear hint of product inhibition control of the reaction. In other words, when the concentration of product in the reaction medium increases, reaction rate sharply decreases, accentuating this behavior as the substrate concentration decreases (which is a sign of competitive inhibition by product) [36]. This behavior reproduces the previously described [33] intrinsic kinetic pattern of the catalysts by the free β-glucosidases. To study this intrinsic kinetic behavior, experiments with the free enzyme batch reactors were performed under the same conditions (Figures S1 and S2, Supplementary Materials) and experimental data for free enzyme were fitted to a kinetic model of substrate-competitive inhibition and product-competitive dual inhibition and different parameters kinetic were obtained (Figure S2, Supplementary Materials). A severe product inhibition was identified, characterized by a low product inhibition constant (K_P = 34.0 mM), and a slight substrate inhibition, characterized by a high substrate inhibition constant (Ki = 1088.1 mM). The Michaelis–Menten constant for the cellobiose was 43.0 mM, indicating a moderate affinity towards the substrate and transition from first order dependency to substrate saturation in the range of usual practical cellobiose concentrations (5–30 g/L). From the quantitative comparison between the initial reaction rate of enzyme-immobilized cellobiose hydrolysis time course (Figure 3) and free-enzyme cellobiose hydrolysis time course (Figure S1), an operational effectiveness factor of 87% for the Ag-PEI biocatalyst and 38% for the Ag-Gly

were obtained. These results are in concordance with the recovered activity reported in Table 1.

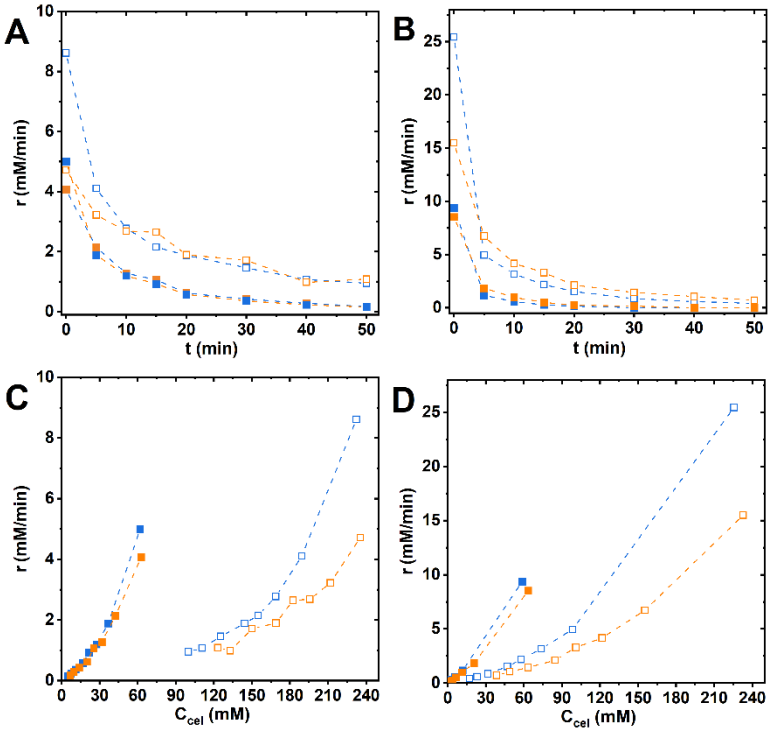

Figure 4. Evolution of the reaction time in the hydrolysis of cellobiose catalyzed by immobilized enzyme. Reaction rate vs. time in the batch reactor (**A**,**B**). Reaction rate vs. cellobiose concentration in the batch reactor (**C**,**D**). All data were obtained by the application of the differential method to the conversion time course of cellobiose catalyzed by different immobilized biocatalysts: Ag-Gly 2000 $U_{\_pNPG}/g_{support}$ (blue squares) and Ag-PEI 2000 $U_{\_pNPG}/g_{support}$ (orange squares), employing different cellobiose concentrations (sodium citrate buffer 50 mM pH 5.0): 20 g/L (filled squares) and 70 g/L (empty squares). The enzyme concentration employed was 0.90 $U_{\_pNPG}$/mL (**A**,**C**) and 4.50 $U_{\_pNPG}$/mL (**B**,**D**).

2.4. From Batch to Continuous: Intensification of Continuous Hydrolysis of Cellobiose Catalyzed by Immobilized β-Glucosidase

Given the inhibition issues of the kinetic, the implementation of the intensified hydrolysis of cellobiose in a continuous reactor requires a careful reaction engineering analysis whereby the reactor format is analyzed in the interplay with the enzyme kinetics. The conversion profile of the cellobiose conversion in a continuous stirred tank reactor and in a tubular reactor is given by Equations (1) and (2) respectively:

$$\tau = \frac{C_{cel_0}}{r} X \tag{1}$$

$$\tau = -\int_{C_{cel_0}}^{C_{cel}} \frac{dC_{cel}}{r} = C_{cel_0} \int_0^x \frac{dX}{r} \tag{2}$$

where r is the kinetic equation defined for MM (Equation (3)) and for the product and substrate inhibition cases (Equation (4)).

$$r = \frac{k_{cat} C_{enz} C_{cel}}{K_M + C_{cel}} \tag{3}$$

$$r = \frac{k_{cat} C_{enz} C_{cel}}{K_M \cdot \left(1 + \frac{2 \cdot \left(C_{cel_0} - C_{cel}\right)}{K_P}\right)^2 + C_{cel} \cdot \left(1 + \frac{C_{cel}}{K_i}\right)} \quad (4)$$

Results were expressed in terms of a dimensionless reaction time, Da_I, that is the first Damköhler (also called number of transfer units, NTU) [51,52], given by the ratio of spatial time and characteristic reaction time, per Equation (5). The characteristic reaction time is given by the ratio of substrate concentration and V_{max} and it indicates the minimum time to reach 100% of conversion if enzyme kinetic would respond to zero order of reaction (K_M very low). The need of $Da_I >>> 1$ is a consequence of high substrate limitation and, especially, high effects of product inhibition.

$$Da_I = \frac{\tau}{\tau_{reac}} = \frac{\tau \, k_{cat} C_{enz}}{C_{cel_0}} \quad (5)$$

Figure 5 shows the simulation of conversion upon variation of the spatial time represented as Da_I. As can be seen, there is high dependence on the conversion profile and reactor/kinetic interplay. While the tubular reactor and MM kinetic allows a high conversion at short time, under the existence of the detected product inhibition, the time should be significantly extended to reach high conversion. In a tubular reactor, the residence time should be 30-fold the intrinsic reaction time to go above 90% of conversion. In the more aggravated case, the CSTR barely reaches 70% with 60 fold. This is a clear manifestation of how the existence of inhibitions per product/substrate significantly affects the conversion achieved in the reactor, showing the expected superiority of the tubular format over the tank format for the continuous operation.

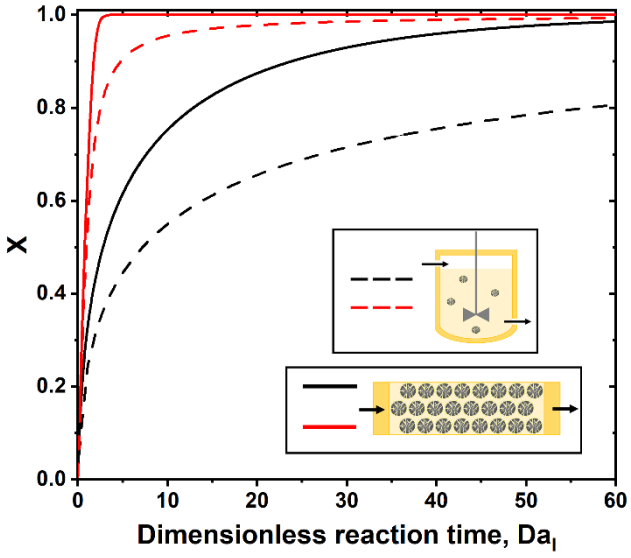

Figure 5. Analysis of conversion of cellobiose dependent on enzyme kinetic, continuous reactor type and residence time. Conversion vs. dimensionless reaction time or first Damköhler number for first order reaction for the CSTR reactor (dashed line) and plug flow/batch reactor (solid line) employing a kinetic model of Michaelis-Menten (red lines) and inhibition acompetitive substrate inhibition and double competitive product inhibition model (black lines). These results were simulated using the kinetics constants obtained for the free enzyme (Table S3, Supplementary Materials) and V_{max} measured for the Ag-Gly 2000 $U_{\_pNPG}/g_{support}$.

Therefore, the implementation of a continuous reactor with immobilized enzymes involved the construction of a fixed-bed reactor. To design the reactor and identify the operation windows, we apply reaction engineering principle and mass balance, as follows. The profile of conversion overtime depends on Equations (1) and (2) and the catalyst load in the reactor. To analyze the maximum achievable productivity and characteristic

reaction time, we have performed analysis for a fixed-bed reactor with different catalyst load ($g_{support}$/mL), as shown in Figure 6. Regarding the operating conditions, the maximum specific productivity was calculated from the measurement of the initial reaction rate with respect to cellobiose as substrate through experiments of hydrolysis of cellobiose in batch reactors to capture the initial rate. This rate was measured at operating temperature (50 °C) and at room temperature, obtaining a maximum specific productivity of 396 mmol/min/$g_{support}$ and 108 mmol/min/$g_{support}$. For both temperatures, we calculated how the amount of enzyme used per reactor volume affected the maximum productivity in the reactor (Figure 6). Maximum productivity in the reactor decreases with temperature (Figure 6), but even at room temperature high productivity is achieved if a high catalyst loading is used. This allows us to operate at a milder temperature even though specific activity is sacrificed, because the conversion would remain high. As the catalyst load increases, the reaction time decreases linearly, allowing to have a characteristic reaction time of one minute in a fixed-bed reactor with maximum catalyst load.

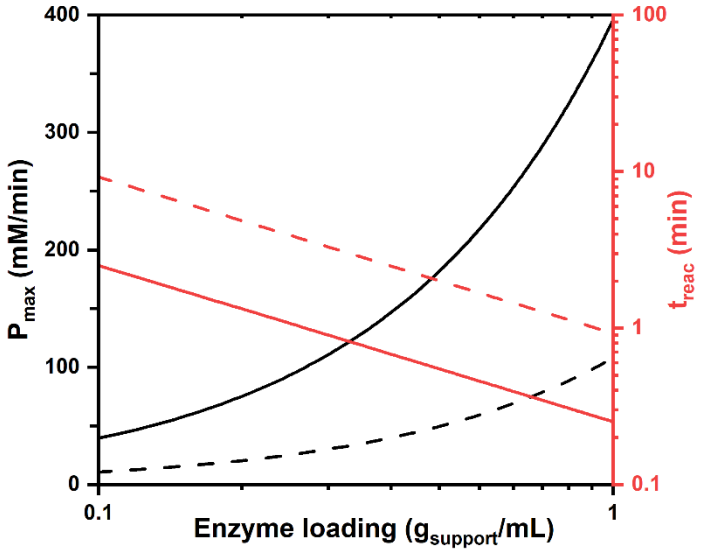

Figure 6. Analysis of the reactor productivity upon variation of catalyst loading and operation temperature. Temperatures: 23.5 °C (solid line) and 50 °C (dashed line). The black line shows the maximum productivity of the immobilized enzyme and the red line shows the time of the reaction. These results were simulated using the kinetics constants obtained for the free enzyme (Table S2, Supplementary Materials) and V_{max} measured for the Ag-Gly 2000 $U_{\_pNPG}/g_{support}$.

Taking the kinetic profile, the catalyst load, and the temperature-dependent activity together, we chose a fixed-bed reactor with full packing of catalyst particles (in the applicable limit of packing agarose and Purolite particles) for the implementation of cellobiose hydrolysis and room temperature as operating conditions. A fixed-bed reactor allows a very high catalyst loading per reactor volume compared to a continuous stirred tank reactor with a distinctive advantage when product inhibition is controlling.

2.5. Implementation of the Hydrolysis of Cellobiose in a Fixed-Bed Continuous Reactor

As a preliminary study, a fixed bed reactor containing immobilized β-glucosidase was implemented and interrogated toward the hydrolysis of pNPG. Different fixed-bed reactors containing Ag-Gly, Ag-PEI, and Pur-Gly were prepared and the performance towards the hydrolysis of 50 mM of pNPG was analyzed. According to catalyst features, the maximum productivity is in the range of 120–970 mM/min and characteristic reaction time fluctuates between 0.1 and 0.83 min. Reactors were operated at different residence times (Da_I 93.9–0.5) until steady state operation was reached (product concentration is constant in the outflow). Product concentration as quantified and results are shown in Figure 7. It was observed (Figure 7) that all the biocatalysts were able to achieve total

conversions employing residence times from 5 to 10 min, except in the case of Ag-PEI biocatalyst (medium load), with conversions achieved between 30% and 60%. Ag-Gly biocatalyst (high load) stood out over the other biocatalyst, achieving 70% conversion in one minute. Notably, the quantification of product formation was disabled in the case of Pur-Gly based reactors as the pNP is strongly retained into the material (results not shown).

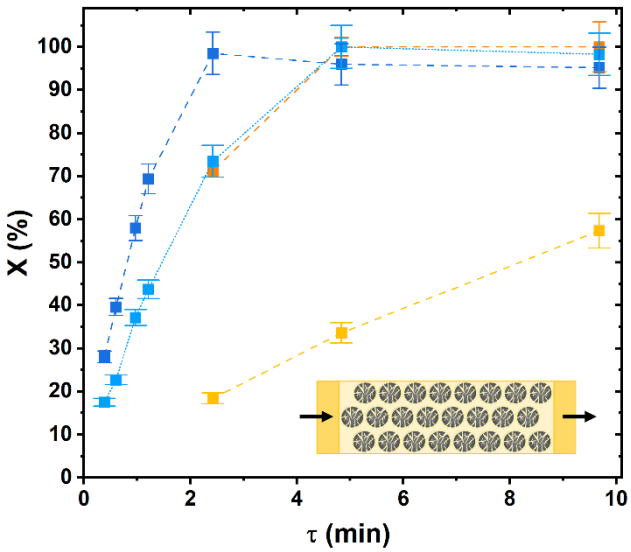

Figure 7. Dependency of the of pNPG conversion with the residence time in fixed-bed reactors containing immobilized enzyme: Ag-Gly 2000 $U_{\_pNPG}/g_{support}$ (dark blue) (t_{reac} = 0.63 min), Ag-Gly 200 $U_{\_pNPG}/g_{support}$ (light blue) (t_{reac} = 0.83 min), Ag-PEI 2000 $U_{\_pNPG}/g_{support}$ (orange) (t_{reac} = 0.1 min), Ag-PEI 200 $U_{\_pNPG}/g_{support}$ (yellow) (t_{reac} = 0.55 min). Data are mean values from multiple experiments (n > 3) under conditions of steady-state and are shown with the calculated SD. All reactions were performed at 22.2 °C employing as substrate a solution of pNPG 50 mM (sodium citrate buffer 100 mM pH 5.0).

After the proof of concept, we apply it to the cellobiose hydrolysis. Founded on the analysis performed in Figures 5 and 6, the reactor was operated with a residence time of 19.4 min. Conversions of nearly 90% were obtained for all biocatalysts, as shown in Figure 8, except for the Ag-PEI of medium loading. No information has been found in the literature about the hydrolysis of cellobiose at room temperature, so these results are interesting from the point of view of the operating conditions. As shown here, even if the temperature is reduced from 50 °C to room temperature, high conversions are still obtained, advancing in an interesting strategy towards the operational stability of the biocatalysts, highly dependent on the operating temperature.

Stability of the different catalysts under operating conditions was analyzed. Reactors were operated for a time span of 8 h, after that, the reactor was disassembled and a sample of the solid catalyst was used to measure the activity, as shown in Figure 9. The Ag-PEI biocatalysts suffered drastic deactivation to about 10% of the initial activity, whereas the Ag-Gly biocatalysts remained at 65% (medium load) and 90% (high load) of the initial activity. This could explain the worse behavior shown by the Ag-PEI biocatalyst in the hydrolysis experiments, since its real activity decreases very quickly during operation. The Ag-Gly (high load) was the biocatalyst that showed the best results with a higher catalytic capacity and greater stability. Based on productivity in the batch reactor, successful full conversion in the fixed-bed reactor, and proven operational stability, the Ag-Gly preparation was the superior catalyst among those tested. The operation time of the reactor described in Figure 8 involves 25 reactor cycles defined as the ratio of operational time and residence (reaction) time. These results agree with those described in the literature for multipoint covalent immobilization [41,53], since although the enzyme activity is much more affected

by immobilization, compared to reversible ionic adsorption, it confers greater operational stability as its tertiary structure is stabilized [19,53].

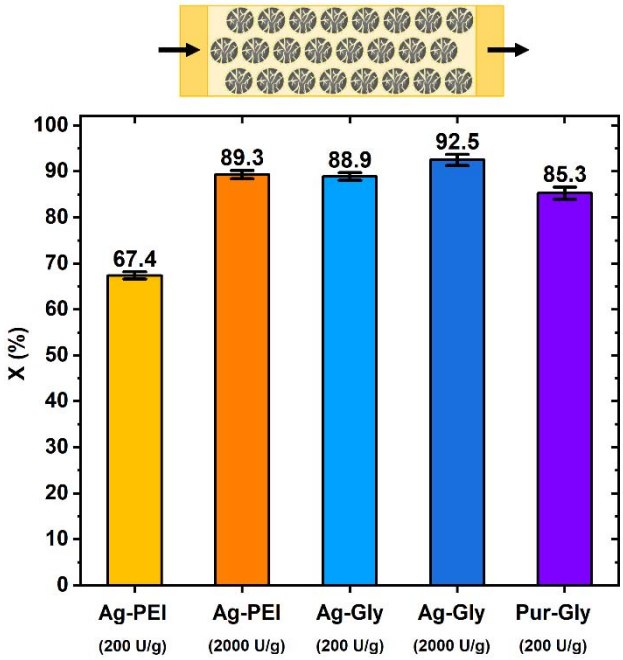

Figure 8. Cellobiose conversion in the operation in fixed-bed reactors containing immobilized enzyme: Ag-Gly 2000 $U_{\_pNPG}/g_{support}$ (dark blue), Ag-Gly 200 $U_{\_pNPG}/g_{support}$ (light blue), Ag-PEI 2000 $U_{\_pNPG}/g_{support}$ (orange), Ag-PEI 200 $U_{\_pNPG}/g_{support}$ (yellow) and Pur-Gly 200 $U_{\_pNPG}/g_{support}$ (purple). All reactions were performed at 23.5 °C with a residence time of 19.4 min employing as substrate a solution of cellobiose 100 mM (sodium citrate buffer 50 mM pH 5.0).

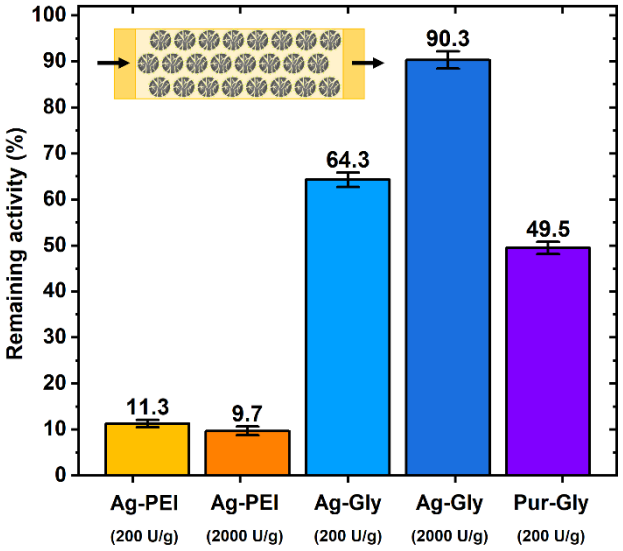

Figure 9. Remaining activity of biocatalysts used in the hydrolysis of cellobiose in continuous operation. In the case of the Pur-Gly biocatalyst, due to the aforementioned adsorption problems, was measured with a dilution of 5 mM pNPG in 100 mM sodium citrate buffer 100 mM pH 5.0 with 30% ethanol to minimize hydrophobic interactions between the matrix and the pNP. The results obtained in the characterization in terms of activity are not valid to this problem of adsorption (Table 1, Section 2.1).

3. Materials and Methods

3.1. Materials

pNPG from Sigma-Aldrich (St. Louis, MO, USA) with a purity of 98% and from AcrosOrganics (Geel, Belgium) with a purity of 99% and cellobiose from Alfa Aesar (Haverhill, MA, USA) were used as substrates. β-glucosidase formulation (β-glucosidase 1000) was a kind donation of ASA Spezialenzyme GmbH (Wolfenbüttel, Germany). The supports used for the immobilization process were Agarose Bead Standard 4% BCL and 6% BCL (Agarose Bead Technologies, Madrid, Spain), which were crosslinked agarose resins with a particle size of 50–150 µm. On the other hand, Purolite Lifetech™ ECR8209F (Purolite, King of Prussia, PA, USA) was used, which is a hydrophilic, medium porosity, methacrylate polymer functionalized with epoxy groups, with a particle size of 150–300 µm. Technical specifications of carrier materials provided by the manufacturer are collected in Table S1. Protein Assay Dye Reagent Concentrate was from (Bio-Rad, Hercules, CA, USA) and BSA from Sigma-Aldrich. Other chemicals were from the analytical grade from Sigma-Aldrich.

3.2. Characterization of Free Enzyme Formulation

The protein content of the enzyme cocktail was evaluated using the Bradford method [54] with commercial Bio-Rad Protein Assay Dye Reagent Concentrate solution and BSA as protein standard solution. Different samples were prepared with different dilutions of enzyme in triplicate. Hence, 20 mL of each sample solution was added to 1 mL of Bradford reagent solution (diluted 1:5) and mixed in the vortex. Mixtures were incubated at room temperature for 15 min and the absorbance of the different samples was measured at 595 nm with a Jasco V-630 spectrophotometer.

3.3. Enzyme Activity Assay

The enzymatic activity for free and immobilized enzyme preparations was evaluated through a colorimetric method. This method is based on the capacity of the enzyme β-glucosidase to hydrolyze pNPG producing pNP and glucose. An enzyme activity unit ($U_{\_pnPG}$) was defined as the amount of enzyme that produces 1 µmol of pNP/min, using as substrate a solution of 5 mM pNPG in 100 mM citrate buffer pH 5.00 at 30 °C. In the case of the free enzyme, 50 µL were added to 1 mL of 5 mM pNPG solution in 100 mM citrate buffer, pH 5.00. In the case of the immobilized biocatalyst, a suspension (100 $mg_{support}/mL_{solution}$) was prepared in 100 mM sodium citrate buffer, pH 5.00. Hence, 50 µL of this suspension were added to 2 mL of 5 mM pNPG solution in 100 mM citrate buffer, pH 5.00. Throughout this process, the sample was kept under constant agitation. pNP release was followed by monitoring the increase of the absorbance (λ = 405 nm) with a Jasco V-360 spectrophotometer, which had a STR-707 water thermostatted cell holder with stirrer to measure the activity of the immobilized enzyme and to maintain a constant temperature. The enzymatic activity was evaluated as the initial reaction rate. The molar extinction coefficient was obtained through the pNP calibration line, resulting in a value of 0.2155 $M^{-1} \cdot cm^{-1}$.

3.4. Enzyme Immobilization

3.4.1. Material Preparation

Activated carrier materials were prepared according to reported procedures. The epoxy-agarose support was prepared as reported by Mateo et al. [55]. The polyethyleneimine activated agarose (Ag-PEI) and polyethyleneimine activated Purolite (Pur-PEI) supports were prepared following a reported procedure [43]. The monoaminoethyl-N-aminoethyl activated agarose (Ag-MANAE) support was prepared as reported [56], using agarose-epoxy instead of agarose-glyoxyl. Glyoxyl activated agarose (Ag-Gly) support was prepared according to protocol described by Guisán [57]. Glyoxyl activated Purolite (Pur-Gly) was prepared by adding 20 g of Purolite to 300 mL of a 0.5 M sulfuric acid solution. The suspension was kept under gentle stirring for 2 h at 25 °C to carry out the oxirane opening. The support was filtered and washed thoroughly with distilled water. For aldehyde generation,

subsequent oxidation with periodate was performed, according to protocol described by Guisán for the preparation of glyoxyl-agarose support from glyceryl support [57]. All the supports were stored at 4 °C until further use.

3.4.2. Reversible Immobilization by Anionic Exchange Ionic Adsorption

For PEI-activated or MANAE-activated material supports, 100 mg support was suspended in 1 mL of enzyme solution in 50 mM sodium phosphate buffer at pH 7.00. The support was previously washed several times with 50 mM sodium phosphate buffer, pH 7.00. Both the free enzyme solution and the support were incubated at room temperature for 15 min under constant gentle stirring (20 rpm) in an end-over-end rotator. Then, the supernatant liquid was extracted, and the immobilized biocatalyst was washed several times with 1 mL/100 $mg_{support}$ of 100 mM sodium citrate buffer pH 5.00 and stored at 4 °C until further use.

3.4.3. Covalent Immobilization

For glyoxyl-activated supports, reported procedures were followed [41]. Thus, 100 mg support was suspended in 1 mL of enzyme solution in 100 mM sodium carbonate buffer at pH 10.05. Both the free enzyme solution and the support were incubated at room temperature for 24 h under constant gentle stirring (20 rpm) in an end-over-end rotator. Then, the supernatant liquid was extracted, and the enzyme derivative was resuspended in 1 mL of immobilization buffer. The biocatalyst was reduced with sodium borohydride (1 mg/mL) for 30 min with constant stirring at 25 °C. Finally, the immobilized biocatalyst was washed several times with 1 mL/100 $mg_{support}$ of 100 mM sodium citrate buffer pH 5.00 and stored at 4 °C until further use.

3.5. Characterization of Immobilized Enzymes

3.5.1. Immobilization

There are different parameters to characterize immobilized biocatalysts, such as immobilization yield, effectiveness factor, and recovered activity [58]. The immobilization yield is the amount of enzyme that is in contact with the support, as the maximum amount of enzyme that can be immobilized (activity offered) [58].

$$Immobilization\ yield = \frac{Offered\ activity - Supernatant\ activity}{Offered\ activity} \quad (6)$$

$$Recovered\ activity = \frac{Observed\ activity}{Offered\ activity} \quad (7)$$

The effectiveness factor is the relation between the observed activity of the biocatalyst and the maximum catalytic activity that the free enzyme would have under the same operating conditions. This maximum activity is calculated by the balance of free enzyme activity.

$$Effectiveness\ factor = \frac{Observed\ activity}{Immobilized\ \ activity} \quad (8)$$

3.5.2. Stability

A defined amount of enzyme immobilized biocatalysts was suspended in 1 mL of 100 mM sodium citrate buffer, pH 5.00. These biocatalysts were incubated in an Eppendorf ThermoMixer® C with constant gentle stirring (300 rpm) at different temperatures (50, 65, and 70 °C). Samples were withdrawn at indicated times and the enzyme activity was measured.

3.5.3. Kinetic Analysis

The variation of the initial reaction rate was studied in the presence of different substrate concentration (pNPG) in 100 mM sodium citrate buffer, pH 5.00. The enzymatic

activity of the different biocatalysts was measured following the pNPG method previously described (Section 3.3).

3.6. Implementation of the Hydrolysis of Cellobiose Enzyme-Immobilized Reactors

3.6.1. Discontinuous Stirred Tank Reactor

The immobilized biocatalysts were incubated with different solutions of cellobiose at different concentrations (20–70 g/L) prepared in 50 mM sodium citrate buffer pH 5.00. The enzyme concentration employed was 0.90 $U_{\_pNPG}$/mL and 4.50 $U_{\_pnPG}$/mL. All experiments were carried out at a temperature of 50 °C and 120 rpm into 100 mL Erlenmeyer flasks with a working volume of 20 mL. A Julabo SW 22 thermostatted bath was used to keep the temperature and agitation constant. Samples (0.5 mL) were collected at different times (0, 5, 10, 15, 20, 30, 40, 50, and 60 min). Absence of enzyme leaching was ensured by submitting the samples to an analysis of hydrolytic activity towards pNPG. These samples were mixed with 0.5 mL of HCl 0.6 M to stop the reaction. Cellobiose and glucose concentration were determined by HPLC (high performance liquid chromatography). HPLC equipment from JASCO (LC-2000 series) was used. This equipment had a column Rezex H+ (300 mm × 7.88 mm), a refraction index detector (RID) RI-2031, a pump PU-2089, an autosampler AS-2059, and a column oven CO-2060. The column was kept at 60 °C, RID detector at 40 °C, and the mobile phase used was acidic water with a sulphuric acid concentration of 5 mM. The pump operated with a flow rate of 0.5 mL/min.

3.6.2. Fixed Bed Reactor

The immobilized biocatalysts were implemented in fixed-bed reactors. In this case, a polypropylene column (EB-Ctg1-5 from Agarose Bead Technologies, Madrid, Spain) with an internal diameter of 6.2 mm and a volume of 1 mL was used. These columns were introduced in a Julabo SW 22 thermostatted bath with temperature and stirring (50 rpm) control. The fixed-bed reactor was washed with 10 mL of 100 mM sodium citrate buffer pH 5.00 using a syringe pump. Absence of enzyme leaching was ensured by submitting the outflow samples to an analysis of hydrolytic activity towards pNPG. After, a sample was taken, and its enzymatic activity was measured to ensure that the enzyme was not desorbing from the support. In the case of the hydrolysis of pNPG, the experiments were carried out at 22.5 °C using a solution of pNPG at 50 mM prepared in 100 mM sodium citrate buffer pH 5.00. A flow rate was set, and samples were taken at different time intervals until the steady state was reached. The pNP concentration was measured by spectrophotometry at 405 nm. This was repeated for different residence times. In the case of enzymatic hydrolysis of cellobiose, experiments were carried out at 23.5 °C using a solution of cellobiose 100 mM in 50 mM sodium citrate buffer pH 5.00. Samples were taken and composition determined by HPLC as described above.

3.7. Kinetic Analysis

For the kinetic analysis, the differential and integration methods were applied. With the differential method, the reaction rate is analyzed as a function of substrate and, if needed, product concentrations (that is, the concentrations of all components that affects the reaction rate). This reaction rate is calculated from concentration–time data through finite increments of reaction time/substrate concentration by obtaining a reaction rate mean value for each time increment. Afterwards, the construction of rate–substrate concentration graphs permits the preliminary selection of the kinetic model by applying a graphical differential method.

In the integral method, we used directly integral data, that is, substrate concentration versus reaction time. In this case, the differential equation relating the reaction rate to kinetic constants and substrate and product concentrations is integrated using a 4th order Runge–Kutta algorithm and parameters are selected by a progressive non-linear regression coupled to such integration. This non-linear regression is based on the Levenberg–Marquardt algorithm. This way, the best values of the kinetic constants are obtained. Berkeley Madonna

software and Aspen Custom Modeler software, where the algorithms are implemented, were used to estimate the different parameters of each kinetic model used to fit the experimental data obtained. Apart from the classical physicochemical criteria (such as the mandatory positive value for the kinetic constants), statistical goodness-of-fit parameters were used to compare different models (the sum of squared errors or sum of variances, SQR, and Fisher's F).

Results were expressed in terms of cellobiose conversion (X) (Equation (9)) and the reaction rate (r, mM/min) (Equation (10)):

$$X = \frac{C_{cel_0} - C_{cel}}{C_{cel_0}} \tag{9}$$

$$r = -\frac{dC_{cel}}{dt} \tag{10}$$

where C_{cel} is the cellobiose concentration at each experimental time (mmol/L) and C_{cel_0} is the initial cellobiose concentration (mmol/L).

The statistical parameters showing the good fitting of the model to experimental data, Fischer's F (F), and sum of quadratic residues (SQR) are given by the following equations:

$$SQR = \sum_{i=1}^{N} \left(y_{i,exp} - y_{i,calc}\right)^2 \tag{11}$$

$$F = \frac{\sum_{i=1}^{N} \frac{(y_{i,calc})^2}{P}}{\sum_{i=1}^{N} \frac{SQR}{N-P}} \tag{12}$$

where N is the number of experiment data and P the number of parameters. In the best case, or for the best kinetic model (if several are compared), when the values calculated with the kinetic model, $y_{i,calc}$, are identical to the experimental values of the variable of interest, $y_{i,exp}$, $SQR \to 0$ and Fisher's F.

4. Conclusions

The design of an active-stable catalyst of β-glucosidase has been achieved by the study and implementation of strategies for binding to porous solid supports. The methodology of multipoint covalent immobilization on glyoxyl activated supports showed a superior performance in terms of catalyst productivity and operational stability. Maximization of enzyme activity was approached, and the catalysts exhibited a high productivity in the hydrolysis of cellulose in discontinuous stirred tank reactors and stability up to 50 °C as an operational condition. Applied kinetics and reaction engineering analysis were integrated in the study of catalyst design and reactor implementation, showing a distinctive advantage for the identification of kinetic bottlenecks and selection of operation conditions. Product inhibition was a key parameter determining the slowing down of the reaction time courses. The simulation of reactor performance under the identified kinetic case allowed us to identify the fixed-bed reactor as a suitable reaction system. Conditions of operation were selected based on previous reactor simulation performance which allowed us to implement 25 °C as working temperature with a maximum catalyst productivity of 109 mmol/min/$g_{support}$. Notwithstanding, the designed catalysts and analysis principles shown here allow us to enhance productivity via tailor-made modification of the reaction conditions. The availability of strategies of biocatalyst design, kinetic models, and reaction engineering analysis offer an interesting toolbox for the design of different strategies of cellulose saccharification to glucose via the sequential, parallel, or integrated application of the different components of the enzymatic breakdown and depolymerization of cellulose: endoglucanases, exoglucanases, and β-glucosidases.

Supplementary Materials: The following supporting information can be downloaded at: https://www.mdpi.com/article/10.3390/catal12010080/s1, Table S1: Technical specifications of material supports used, Table S2: Fitting of the activity time course of beta-glucosidase catalysts, Table S3: Kinetic and statistical parameters of the different fittings of the kinetic models, Figure S1: Conversion time course of the hydrolysis of cellobiose catalyzed by free enzyme, Figure S2: Reaction rate evolution of the hydrolysis of cellobiose catalyzed by free enzyme.

Author Contributions: Conceptualization, M.L. and J.M.B.; methodology, C.A.-G., M.L. and J.M.B.; data analysis, C.A.-G.; investigation, C.A.-G. and J.M.B.; resources, V.E.S., M.L. and J.M.B.; data curation, C.A.-G., V.E.S., M.L. and J.M.B.; writing—original draft preparation, C.A.-G. and J.M.B.; writing—review and editing, C.A.-G., M.L. and J.M.B.; supervision, V.E.S., M.L. and J.M.B.; project administration and funding acquisition, V.E.S., M.L. and J.M.B. All authors have read and agreed to the published version of the manuscript.

Funding: J.M.B. acknowledges funding from the Government of Community of Madrid (2018-T1/BIO-10200). C.A.-G., V.E.S. and M.L.G. gratefully acknowledge funding by MINECO via projects CTQ2017-84963-C2-1-R and PCI2018-093114.

Data Availability Statement: All relevant data is contained in the manuscript and Supplementary Materials.

Conflicts of Interest: The authors declare no conflict of interest. The funders had no role in the design of the study; in the collection, analyses, or interpretation of data; in the writing of the manuscript, or in the decision to publish the results.

References

1. Venkata Mohan, S.; Dahiya, S.; Amulya, K.; Katakojwala, R.; Vanitha, T.K. Can Circular Bioeconomy Be Fueled by Waste Biorefineries—A Closer Look. *Bioresour. Technol. Rep.* **2019**, *7*, 100277. [CrossRef]
2. Mak, T.M.W.; Xiong, X.; Tsang, D.C.W.; Yu, I.K.M.; Poon, C.S. Sustainable Food Waste Management towards Circular Bioeconomy: Policy Review, Limitations and Opportunities. *Bioresour. Technol.* **2020**, *297*, 122497. [CrossRef]
3. Ubando, A.T.; Felix, C.B.; Chen, W.-H. Biorefineries in Circular Bioeconomy: A Comprehensive Review. *Bioresour. Technol.* **2020**, *299*, 122585. [CrossRef]
4. Cantzler, J.; Creutzig, F.; Ayargarnchanakul, E.; Javaid, A.; Wong, L.; Haas, W. Saving Resources and the Climate? A Systematic Review of the Circular Economy and Its Mitigation Potential. *Environ. Res. Lett.* **2020**, *15*, 123001. [CrossRef]
5. Garcia-Ochoa, F.; Vergara, P.; Wojtusik, M.; Gutiérrez, S.; Santos, V.E.; Ladero, M.; Villar, J.C. Multi-Feedstock Lignocellulosic Biorefineries Based on Biological Processes: An Overview. *Ind. Crops Prod.* **2021**, *172*, 114062. [CrossRef]
6. Vu, H.P.; Nguyen, L.N.; Vu, M.T.; Johir, M.A.H.; McLaughlan, R.; Nghiem, L.D. A Comprehensive Review on the Framework to Valorise Lignocellulosic Biomass as Biorefinery Feedstocks. *Sci. Total Environ.* **2020**, *743*, 140630. [CrossRef]
7. Méndez-Líter, J.A.; Gil-Muñoz, J.; Nieto-Domínguez, M.; Barriuso, J.; de Eugenio, L.I.; Martínez, M.J. A Novel, Highly Efficient β-Glucosidase with a Cellulose-Binding Domain: Characterization and Properties of Native and Recombinant Proteins. *Biotechnol. Biofuels* **2017**, *10*, 256. [CrossRef] [PubMed]
8. Li, X.; Xiao, Y.; Feng, Y.; Li, B.; Li, W.; Cui, Q. The Spatial Proximity Effect of Beta-Glucosidase and Cellulosomes on Cellulose Degradation. *Enzym. Microb. Technol.* **2018**, *115*, 52–61. [CrossRef]
9. Wang, Y.; Milewska, M.; Foster, H.; Chapman, R.; Stenzel, M.H. The Core–Shell Structure, Not Sugar, Drives the Thermal Stabilization of Single-Enzyme Nanoparticles. *Biomacromolecules* **2021**, *22*, 4569–4581. [CrossRef] [PubMed]
10. Wojtusik, M.; Vergara, P.; Villar, J.C.; Garcia-Ochoa, F.; Ladero, M. Thermal and Operational Deactivation of Aspergillus Fumigatus β-Glucosidase in Ethanol/Water Pretreated Wheat Straw Enzymatic Hydrolysis. *J. Biotechnol.* **2019**, *292*, 32–38. [CrossRef]
11. Andrić, P.; Meyer, A.S.; Jensen, P.A.; Dam-Johansen, K. Reactor Design for Minimizing Product Inhibition during Enzymatic Lignocellulose Hydrolysis: I. Significance and Mechanism of Cellobiose and Glucose Inhibition on Cellulolytic Enzymes. *Biotechnol. Adv.* **2010**, *28*, 308–324. [CrossRef]
12. Huang, C.; Feng, Y.; Patel, G.; Xu, X.; Qian, J.; Liu, Q.; Kai, G. Production, Immobilization and Characterization of Beta-Glucosidase for Application in Cellulose Degradation from a Novel Aspergillus Versicolor. *Int. J. Biol. Macromol.* **2021**, *177*, 437–446. [CrossRef]
13. Uchiyama, T.; Miyazaki, K.; Yaoi, K. Characterization of a Novel β-Glucosidase from a Compost Microbial Metagenome with Strong Transglycosylation Activity. *J. Biol. Chem.* **2013**, *288*, 18325–18334. [CrossRef]
14. Sørensen, A.; Lübeck, M.; Lübeck, P.; Ahring, B. Fungal Beta-Glucosidases: A Bottleneck in Industrial Use of Lignocellulosic Materials. *Biomolecules* **2013**, *3*, 612–631. [CrossRef]
15. Srivastava, N.; Rathour, R.; Jha, S.; Pandey, K.; Srivastava, M.; Thakur, V.K.; Sengar, R.S.; Gupta, V.K.; Mazumder, P.B.; Khan, A.F.; et al. Microbial Beta Glucosidase Enzymes: Recent Advances in Biomass Conversation for Biofuels Application. *Biomolecules* **2019**, *9*, 220. [CrossRef]

16. Singhania, R.R.; Patel, A.K.; Sukumaran, R.K.; Larroche, C.; Pandey, A. Role and Significance of Beta-Glucosidases in the Hydrolysis of Cellulose for Bioethanol Production. *Bioresour. Technol.* **2013**, *127*, 500–507. [CrossRef]
17. Andrades, D.; Graebin, N.G.; Ayub, M.A.Z.; Fernandez-Lafuente, R.; Rodrigues, R.C. Preparation of Immobilized/Stabilized Biocatalysts of B-glucosidases from Different Sources: Importance of the Support Active Groups and the Immobilization Protocol. *Biotechnol. Prog.* **2019**, *35*. [CrossRef] [PubMed]
18. Andrades, D.; Graebin, N.G.; Ayub, M.A.Z.; Fernandez-Lafuente, R.; Rodrigues, R.C. Physico-Chemical Properties, Kinetic Parameters, and Glucose Inhibition of Several Beta-Glucosidases for Industrial Applications. *Process Biochem.* **2019**, *78*, 82–90. [CrossRef]
19. Rodrigues, R.C.; Ortiz, C.; Berenguer-Murcia, Á.; Torres, R.; Fernández-Lafuente, R. Modifying Enzyme Activity and Selectivity by Immobilization. *Chem. Soc. Rev.* **2013**, *42*, 6290–6307. [CrossRef] [PubMed]
20. Guisan, J.M.; López-Gallego, F.; Bolivar, J.M.; Rocha-Martín, J.; Fernandez-Lorente, G. The Science of Enzyme Immobilization. In *Immobilization of Enzymes and Cells*; Guisan, J.M., Bolivar, J.M., López-Gallego, F., Rocha-Martín, J., Eds.; Springer: New York, NY, USA, 2020; Volume 2100, pp. 1–26, ISBN 978-1-07-160214-0.
21. Bolivar, J.M.; Eisl, I.; Nidetzky, B. Advanced Characterization of Immobilized Enzymes as Heterogeneous Biocatalysts. *Catal. Today* **2016**, *259*, 66–80. [CrossRef]
22. Valikhani, D.; Bolivar, J.M.; Pelletier, J.N. An Overview of Cytochrome P450 Immobilization Strategies for Drug Metabolism Studies, Biosensing, and Biocatalytic Applications: Challenges and Opportunities. *ACS Catal.* **2021**, *11*, 9418–9434. [CrossRef]
23. Garcia-Galan, C.; Berenguer-Murcia, Á.; Fernandez-Lafuente, R.; Rodrigues, R.C. Potential of Different Enzyme Immobilization Strategies to Improve Enzyme Performance. *Adv. Synth. Catal.* **2011**, *353*, 2885–2904. [CrossRef]
24. Jung, Y.R.; Shin, H.Y.; Song, Y.S.; Kim, S.B.; Kim, S.W. Enhancement of Immobilized Enzyme Activity by Pretreatment of β-Glucosidase with Cellobiose and Glucose. *J. Ind. Eng. Chem.* **2012**, *18*, 702–706. [CrossRef]
25. Ahirwar, R.; Sharma, J.G.; Nahar, P.; Kumar, S. Immobilization Studies of Cellulase on Three Engineered Polymer Surfaces. *Biocatal. Agric. Biotechnol.* **2017**, *11*, 248–251. [CrossRef]
26. Morais Junior, W.G.; Pacheco, T.F.; Gao, S.; Martins, P.A.; Guisán, J.M.; Caetano, N.S. Sugarcane Bagasse Saccharification by Enzymatic Hydrolysis Using Endocellulase and β-Glucosidase Immobilized on Different Supports. *Catalysts* **2021**, *11*, 340. [CrossRef]
27. Ahmed, S.A.; El-Shayeb, N.M.A.; Hashem, A.M.; Saleh, S.A.; Abdel-Fattah, A.F. Biochemical Studies on Immobilized Fungal β-Glucosidase. *Braz. J. Chem. Eng.* **2013**, *30*, 747–758. [CrossRef]
28. Figueira, J.A.; Dias, F.F.G.; Sato, H.H.; Fernandes, P. Screening of Supports for the Immobilization of β-Glucosidase. *Enzym. Res.* **2011**, *2011*, 642460. [CrossRef] [PubMed]
29. Piñuel, L.; Mazzaferro, L.S.; Breccia, J.D. Operational Stabilization of Fungal α-Rhamnosyl-β-Glucosidase by Immobilization on Chitosan Composites. *Process Biochem.* **2011**, *46*, 2330–2335. [CrossRef]
30. Califano, V.; Costantini, A.; Silvestri, B.; Venezia, V.; Cimino, S.; Sannino, F. The Effect of Pore Morphology on the Catalytic Performance of β-Glucosidase Immobilized into Mesoporous Silica. *Pure Appl. Chem.* **2019**, *91*, 1583–1592. [CrossRef]
31. Wu, X.; Qu, B.; Liu, Y.; Ren, X.; Wang, S.; Quan, Y. Highly Enhanced Activity and Stability via Affinity Induced Immobilization β-Glucosidase from Aspergillus Niger onto Amino-Based Silica for the Biotransformation of Ginsenoside Rb1. *J. Chromatogr. A* **2021**, *1653*, 462388. [CrossRef]
32. Alftrén, J.; Hobley, T.J. Covalent Immobilization of β-Glucosidase on Magnetic Particles for Lignocellulose Hydrolysis. *Appl. Biochem. Biotechnol.* **2013**, *169*, 2076–2087. [CrossRef] [PubMed]
33. Wojtusik, M.; Yepes, C.M.; Villar, J.C.; Cordes, A.; Arroyo, M.; Garcia-Ochoa, F.; Ladero, M. Kinetic Modeling of Cellobiose by a β-Glucosidase from Aspergillus Fumigatus. *Chem. Eng. Res. Des.* **2018**, *136*, 502–512. [CrossRef]
34. Dias Gomes, M.; Woodley, J.M. Considerations When Measuring Biocatalyst Performance. *Molecules* **2019**, *24*, 3573. [CrossRef] [PubMed]
35. Kuusk, S.; Väljamäe, P. When Substrate Inhibits and Inhibitor Activates: Implications of β-Glucosidases. *Biotechnol. Biofuels* **2017**, *10*, 7. [CrossRef]
36. Lorente-Arevalo, A.; Garcia-Martin, A.; Ladero, M.; Bolivar, J.M. Chemical Reaction Engineering to Understand Applied Kinetics in Free Enzyme Homogeneous Reactors. In *Enzyme Engineering*; Magnani, F., Marabelli, C., Paradisi, F., Eds.; Methods in Molecular Biology; Springer: New York, NY, USA, 2022; Volume 2397, pp. 277–320, ISBN 978-1-07-161825-7.
37. Venezia, V.; Califano, V.; Pota, G.; Costantini, A.; Landi, G.; Di Benedetto, A. CFD Simulations of Microreactors for the Hydrolysis of Cellobiose to Glucose by β-Glucosidase Enzyme. *Micromachines* **2020**, *11*, 790. [CrossRef] [PubMed]
38. Venezia, V.; Costantini, A.; Landi, G.; Di Benedetto, A.; Sannino, F.; Califano, V. Immobilization of β-Glucosidase over Structured Cordierite Monoliths Washcoated with Wrinkled Silica Nanoparticles. *Catalysts* **2020**, *10*, 889. [CrossRef]
39. Wei, C.; Zhou, Y.; Zhuang, W.; Li, G.; Jiang, M.; Zhang, H. Improving the Performance of Immobilized β-Glucosidase Using a Microreactor. *J. Biosci. Bioeng.* **2018**, *125*, 377–384. [CrossRef] [PubMed]
40. Santos, J.C.S.; Barbosa, O.; Ortiz, C.; Berenguer-Murcia, A.; Rodrigues, R.C.; Fernandez-Lafuente, R. Importance of the Support Properties for Immobilization or Purification of Enzymes. *ChemCatChem* **2015**, *7*, 2413–2432. [CrossRef]

41. López-Gallego, F.; Fernandez-Lorente, G.; Rocha-Martín, J.; Bolivar, J.M.; Mateo, C.; Guisan, J.M. Multi-Point Covalent Immobilization of Enzymes on Glyoxyl Agarose with Minimal Physico-Chemical Modification: Stabilization of Industrial Enzymes. In *Immobilization of Enzymes and Cells*; Guisan, J.M., Bolivar, J.M., López-Gallego, F., Rocha-Martín, J., Eds.; Methods in Molecular Biology; Springer: New York, NY, USA, 2020; Volume 2100, pp. 93–107, ISBN 978-1-07-160214-0.
42. Mateo, C.; Palomo, J.M.; Fuentes, M.; Betancor, L.; Grazu, V.; López-Gallego, F.; Pessela, B.C.C.; Hidalgo, A.; Fernández-Lorente, G.; Fernández-Lafuente, R.; et al. Glyoxyl Agarose: A Fully Inert and Hydrophilic Support for Immobilization and High Stabilization of Proteins. *Enzym. Microb. Technol.* **2006**, *39*, 274–280. [CrossRef]
43. Mateo, C.; Abian, O.; Fernandez-Lafuente, R.; Guisan, J.M. Reversible Enzyme Immobilization via a Very Strong and Nondistorting Ionic Adsorption on Support-Polyethylenimine Composites. *Biotechnol. Bioeng.* **2000**, *68*, 98–105. [CrossRef]
44. Virgen-Ortíz, J.J.; dos Santos, J.C.S.; Berenguer-Murcia, Á.; Barbosa, O.; Rodrigues, R.C.; Fernandez-Lafuente, R. Polyethylenimine: A Very Useful Ionic Polymer in the Design of Immobilized Enzyme Biocatalysts. *J. Mater. Chem. B* **2017**, *5*, 7461–7490. [CrossRef]
45. Vieira, M.F.; Vieira, A.M.S.; Zanin, G.M.; Tardioli, P.W.; Mateo, C.; Guisán, J.M. β-Glucosidase Immobilized and Stabilized on Agarose Matrix Functionalized with Distinct Reactive Groups. *J. Mol. Catal. B Enzym.* **2011**, *69*, 47–53. [CrossRef]
46. Vazquez-Ortega, P.G.; Alcaraz-Fructuoso, M.T.; Rojas-Contreras, J.A.; López-Miranda, J.; Fernandez-Lafuente, R. Stabilization of Dimeric β-Glucosidase from Aspergillus Niger via Glutaraldehyde Immobilization under Different Conditions. *Enzym. Microb. Technol.* **2018**, *110*, 38–45. [CrossRef]
47. Da Silva, T.M.; Pessela, B.C.; da Silva, J.C.R.; Lima, M.S.; Jorge, J.A.; Guisan, J.M.; Maria de Lourdes, T.M. Immobilization and High Stability of an Extracellular β-Glucosidase from Aspergillus Japonicus by Ionic Interactions. *J. Mol. Catal. B Enzym.* **2014**, *104*, 95–100. [CrossRef]
48. De Andrades, D.; Graebin, N.G.; Kadowaki, M.K.; Ayub, M.A.Z.; Fernandez-Lafuente, R.; Rodrigues, R.C. Immobilization and Stabilization of Different β-Glucosidases Using the Glutaraldehyde Chemistry: Optimal Protocol Depends on the Enzyme. *Int. J. Biol. Macromol.* **2019**, *129*, 672–678. [CrossRef] [PubMed]
49. Teixeira da Silva, V.C.; de Souza Coto, A.L.; de Carvalho Souza, R.; Bertoldi Sanchez Neves, M.; Gomes, E.; Bonilla-Rodriguez, G.O. Effect of pH, Temperature, and Chemicals on the Endoglucanases and β-Glucosidases from the Thermophilic Fungus Myceliophthora Heterothallica F.2.1.4. Obtained by Solid-State and Submerged Cultivation. *Biochem. Res. Int.* **2016**, *2016*, 9781216. [CrossRef] [PubMed]
50. Liu, D.; Zhang, R.; Yang, X.; Zhang, Z.; Song, S.; Miao, Y.; Shen, Q. Characterization of a Thermostable β-Glucosidase from Aspergillus Fumigatus Z5, and Its Functional Expression in Pichia Pastoris X33. *Microb. Cell Fact.* **2012**, *11*, 25. [CrossRef] [PubMed]
51. Bolivar, J.M.; Tribulato, M.A.; Petrasek, Z.; Nidetzky, B. Let the Substrate Flow, Not the Enzyme: Practical Immobilization of d-Amino Acid Oxidase in a Glass Microreactor for Effective Biocatalytic Conversions. *Biotechnol. Bioeng.* **2016**, *113*, 2342–2349. [CrossRef]
52. Bolivar, J.M.; Valikhani, D.; Nidetzky, B. Demystifying the Flow: Biocatalytic Reaction Intensification in Microstructured Enzyme Reactors. *Biotechnol. J.* **2019**, *14*, 1800244. [CrossRef]
53. Mateo, C.; Palomo, J.M.; Fernandez-Lorente, G.; Guisan, J.M.; Fernandez-Lafuente, R. Improvement of Enzyme Activity, Stability and Selectivity via Immobilization Techniques. *Enzym. Microb. Technol.* **2007**, *40*, 1451–1463. [CrossRef]
54. Bradford, M.M. A Rapid and Sensitive Method for the Quantitation of Microgram Quantities of Protein Utilizing the Principle of Protein-Dye Binding. *Anal. Biochem.* **1976**, *72*, 248–254. [CrossRef]
55. Mateo, C.; Bolivar, J.M.; Godoy, C.A.; Rocha-Martin, J.; Pessela, B.C.; Curiel, J.A.; Muñoz, R.; Guisan, J.M.; Fernández-Lorente, G. Improvement of Enzyme Properties with a Two-Step Immobilizaton Process on Novel Heterofunctional Supports. *Biomacromolecules* **2010**, *11*, 3112–3117. [CrossRef] [PubMed]
56. Fernandez-Lafuente, R.; Rosell, C.M.; Rodriguez, V.; Santana, C.; Soler, G.; Bastida, A.; Guisán, J.M. Preparation of Activated Supports Containing Low PK Amino Groups. A New Tool for Protein Immobilization via the Carboxyl Coupling Method. *Enzym. Microb. Technol.* **1993**, *15*, 546–550. [CrossRef]
57. Guisán, J.M. Aldehyde-Agarose Gels as Activated Supports for Immobilization-Stabilization of Enzymes. *Enzym. Microb. Technol.* **1988**, *10*, 375–382. [CrossRef]
58. Illanes, A.; Wilson, L.; Vera, C. Enzyme Kinetics in a Heterogeneous System. In *Problem Solving in Enzyme Biocatalysis*; John Wiley and Sons Ltd.: Chichester, UK, 2013; pp. 87–140, ISBN 978-1-118-34174-2.